Hindawi Publishing Corporation
International Journal of Carbohydrate Chemistry
Volume 2009, Article ID 307695, 8 pages
doi:10.1155/2009/307695

Research Article

On the Conformational Properties of Amylose and Cellulose Oligomers in Solution

Moritz Winger, Markus Christen, and Wilfred F. van Gunsteren

Laboratory of Physical Chemistry, Swiss Federal Institute of Technology Zürich, ETH, 8093 Zürich, Switzerland

Correspondence should be addressed to Wilfred F. van Gunsteren, wfvgn@igc.phys.chem.ethz.ch

Received 23 October 2008; Revised 10 February 2009; Accepted 1 April 2009

Recommended by Robert J. Woods

Molecular dynamics (MD) simulations were used to monitor the stability and conformation of double-stranded and single-stranded amyloses and single-stranded cellulose oligomers containing 9 sugar moieties in solution as a function of solvent composition, ionic strength, temperature, and methylation state. This study along with other previous studies suggests that hydrogen bonds are crucial for guaranteeing the stability of the amylose double helix. Single-stranded amylose forms a helical structure as well, and cellulose stays highly elongated throughout the simulation time, a behavior that was also observed experimentally. In terms of coordination of solute hydroxyl groups with ions, amylose shows entropy-driven coordination of calcium and sulfate ions, whereas cellulose-ion coordination seems to be enthalpy-dominated. This indicates that entropy considerations cannot be neglected when explaining the structural differences between amyloses and celluloses.

1. Introduction

Amylose and cellulose are linear polymers of glucose linked with 1,4-bonds. The main difference is the anomeric configureration: amylose's glucose units are linked with $\alpha(1 \rightarrow 4)$ glycosidic bonds, whereas cellulose's monomeric units are linked by $\beta(1 \rightarrow 4)$ glycosidic bonds. This different kind of bonding causes amylose to form helical structures and cellulose to form straight polymer chains.

Amylose occurs in different forms, the A, B, V, and other forms [1]. The A and B forms both feature left-handed helices with six glucose units per turn and seem to differ only in the packing of the starch helices. The V form of amylose is obtained through cocrystallization with compounds such as iodine, DMSO, alcohols, or fatty acids [2, 3]. The helical conformations of B- and V-amylose show differences [4–6].

Cellulose is a linear polymer and is the most abundant natural polymer on earth. Cellulose's structure and properties have been investigated extensively, but still there are uncertainties about cellulose's crystal structure [7–9]. X-ray scattering and electron diffraction experiments show that cellulose forms aggregates to sheet-like structures with the cellulose molecules in elongated conformation.

These structural differences are the reason why amyloses and celluloses have very different physical and biological properties [10]. Amylose is poorly soluble in water and forms suspensions, in which its helicity is preserved. Cellulose fibers are insoluble in water.

Computer simulations of these systems can be done to get atomic-level insight into the behavior of these molecules and to perform computational studies of their properties. A Monte-Carlo computer simulation of double-helical amylose in water by Eisenhaber and Schuler [11] suggests that a left-handed antiparallel double helix fits best to the structure of liquid water. Regular water bridges forming a network around the duplex were observed.

Previous molecular dynamics (MD) studies on amylose and cellulose have been done by Yu et al. [12]. Fragments of these molecules were methylated at different positions, and their stabilities were monitored. The authors concluded that single helices are more destabilized by methylation of amylose's O-2 and O-3 moieties than by methylation at O-6 , but that the methylation of O-6 destabilizes double helices more.

In the present work simulations of double-stranded and single-stranded amyloses and single-stranded cellulose

Table 1: Overview of the performed MD simulations of the different double-stranded (dou) or single-stranded (sin) carbohydrate systems: amylose (amy) and cellulose (cel).

Simulation label	Simulated system	Number of solvent molecules	Solvent	T/K	Number of counterions	Simulation length/ns
amy_dou_H_2O	amy	3633	H_2O	313	0	5.5
amy_noHB_dou_H_2O	amy hydrogen bonds excluded	3633	H_2O	313	0	2.1
amy_met_dou_H_2O	amy methylated	3633	H_2O	313	0	5.5
amy_dou_DMSO	amy	937	DMSO	313	0	5.2
amy_met_dou_DMSO	amy methylated	937	DMSO	313	0	7
amy_dou_H_2O_caso	amy	3613	H_2O	313	10 Ca^{2+}, 10 SO_4^{2-}	7
amy_sin_H_2O_caso	single-stranded amy	3613	H_2O	278/313	10 Ca^{2+}, 10 SO_4^{2-}	8
cel_sin_H_2O_caso	single-stranded cel	3617	H_2O	278/313	8 Ca^{2+}, 8 SO_4^{2-}	10

oligomers consisting of 9 sugar moieties are analyzed, and the stability of particular structures of these molecules is studied as a function of type of solvent, ionic strength, temperature, and methylation state.

2. Methods

2.1. Molecular Dynamics Simulations. MD simulations were performed with the GROMOS software package [13–15] using the force-field parameter set 53A6 [16], which treats aliphatic carbons as united atoms. Sugar parameters have been optimized for the GROMOS force field by Lins and Hünenberger [17]. The MD simulations performed for molecules consisting of 9 sugar units are summarized in Table 1. Amylose's and cellulose's initial coordinates were generated with the INSIGHTII software package (Accelerys Inc., San Diego, Calif, USA). Amylose was modeled into a double helix. Initial solute conformations of the amylose double-helix were the regular helices built from the data by Imberty et al. [18]. This model is characterized by torsional angles of $\phi = \angle(O5, C1, O4', C4') = 84°$ and $\psi = \angle(C1, O4', C4', C5') = -145°$. To further investigate the role of hydrogen bonds in helix stability, simulations with all nonbonded interactions between solute atoms involved in hydrogen bonds turned off were carried out (label: noHB) as well as simulations with hydroxy-groups involved in hydrogen bonds methylated (label: met). In the topologies for the simulations with excluded hydrogen bonds, Lennard-Jones interactions between hydrogen-bonded atoms have been set to zero. For the simulations of single-stranded amylose one strand was removed from the double-helical starting structure. The simulations involving cellulose oligomers started from an extended conformation with the angles $\phi = -120°$ and $\psi = -120°$. The simple-point-charge (SPC) water model [19] was used to describe the solvent molecules. In some simulations DMSO [20] was used as a solvent (label: DMSO). In the simulations the solvent molecules were added around the solute within a rectangular box for (double-stranded) amylose and cellulose with a minimum distance of 1.4 nm between the solute atoms and the walls of the periodic box. In the simulations roto-translational constraints have been used [21]. In some of the simulations in aqueous solution, ions (SO_4^{2-} and Ca^{2+}) were included (Table 1). The initial placement of the ions was random. All the bonds and the bond angles of the solvent molecules were constrained with a geometric tolerance of 10^{-4} using the SHAKE algorithm [22]. The steepest-descent energy minimization without any restraints of all systems was performed to relax the solute-solvent contacts. The energy minimizations were terminated when the energy change per step became smaller than 0.1 kJ mol^{-1}. For the nonbonded interactions, a triple-range method with cutoff radii of 0.8/1.4 nm was used. Short-range van der Waals and electrostatic interactions were evaluated every (time) step based on a charge-group pairlist. Medium-range van der Waals and electrostatic interactions, between pairs at a distance longer than 0.8 nm and shorter than 1.4 nm, were evaluated every fifth (time) step, at which (time) point the pair list was updated. Outside the longer cutoff radius a reaction-field approximation [23] was used with a relative dielectric permittivity of 66 [24]. The initial velocities of the atoms were assigned from a Maxwell distribution at 50 K. For amylose four 50 ps periods of MD simulation with harmonic position restraining of the solute atoms with force constants of $1.0 \cdot 10^4$ kJ mol^{-1} nm^{-2}, $1.0 \cdot 10^3$ kJ mol^{-1} nm^{-2}, $1.0 \cdot 10^2$ kJ mol^{-1} nm^{-2}, and 5.0 kJ mol^{-1} nm^{-2} were performed to equilibrate further the systems at 50 K, 100 K, 200 K, and 278/313 K, respectively. For cellulose five 50 ps periods of MD simulation with harmonic position restraining of the solute atoms with force constants of $2.5 \cdot 10^4$ kJ mol^{-1} nm^{-2}, $1.0 \cdot 10^4$ kJ mol^{-1} nm^{-2}, $1.0 \cdot 10^3$ kJ mol^{-1} nm^{-2}, $1.0 \cdot 10^2$ kJ mol^{-1} nm^{-2}, and 5.0 kJ mol^{-1} nm^{-2} were performed to equilibrate further the systems at 50 K, 100 K, 200 K, 278/313 K, and 278/313 K, respectively. During the equilibration, solvent and solute degrees of freedom were independently, weakly coupled to a temperature bath at the given temperature with a relaxation time of 0.1 ps [25]. In the further simulations, the center of mass motion of the whole system was set to zero every 1000 time steps. The systems were also weakly coupled to a pressure bath of 1 atom with a relaxation time of 0.5 ps and an isothermal compressibility of

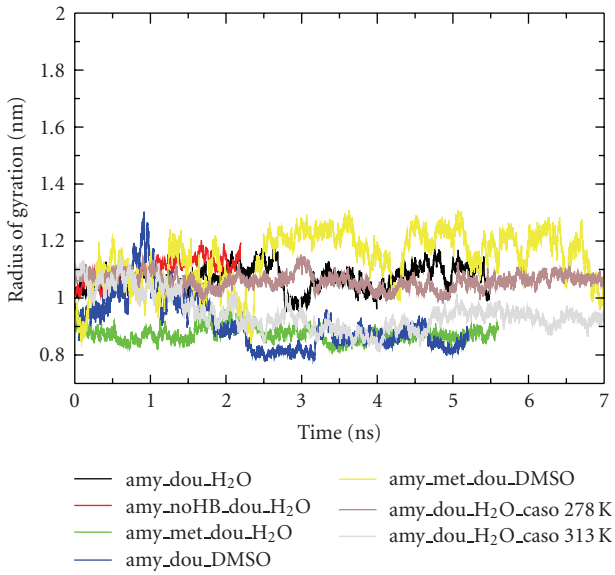

FIGURE 1: Radius of gyration as function of time for the simulations of double-stranded amylose under various conditions, such as different temperatures, solvents, ionic strengths, and methylation states. The labels of the simulations are defined in Table 1.

0.4575×10^{-3} (kJ mol^{-1} nm^{-3})$^{-1}$. The trajectory coordinates and energies were saved every 0.5 ps for analysis.

2.2. Analysis. Analyses were done with the analysis software packages GROMOS++ [15] and esra [26]. Radii of gyration were calculated to observe the level of compactness of the simulated molecules. Structural information on ionic solutions was obtained from the radial distribution functions $g(r)$. For amylose, percentages of inter- and intramolecular hydrogen bonds were calculated using a maximum distance criterion of 0.25 nm between the hydrogen atom and the acceptor atom and a minimum angle criterion of 135° for the donor-hydrogen-acceptor angle.

3. Results

3.1. Double-Stranded Amylose in Pure Solvent. The radii of gyration of amylose in different solvents and methylation states are shown in Figure 1. Exclusion of interactions between atoms that form hydrogen bonds do not influence the behavior of the radii of gyration significantly. Hydrogen bond percentages are shown in Table 2. Excluding the hydrogen bond interaction in the simulation makes hydrogen bonds as analyzed vanish. Simulating in DMSO increases the solute-solute hydrogen bonding, and higher percentages can be observed. Methylation of the structure reduces solute-solute hydrogen bonding to zero. Still the structures of the methylated and unmethylated cases yield similar radii of gyration (Figure 1). Their structures are different, however, comparing the final structures (Figure 2). Amylose with

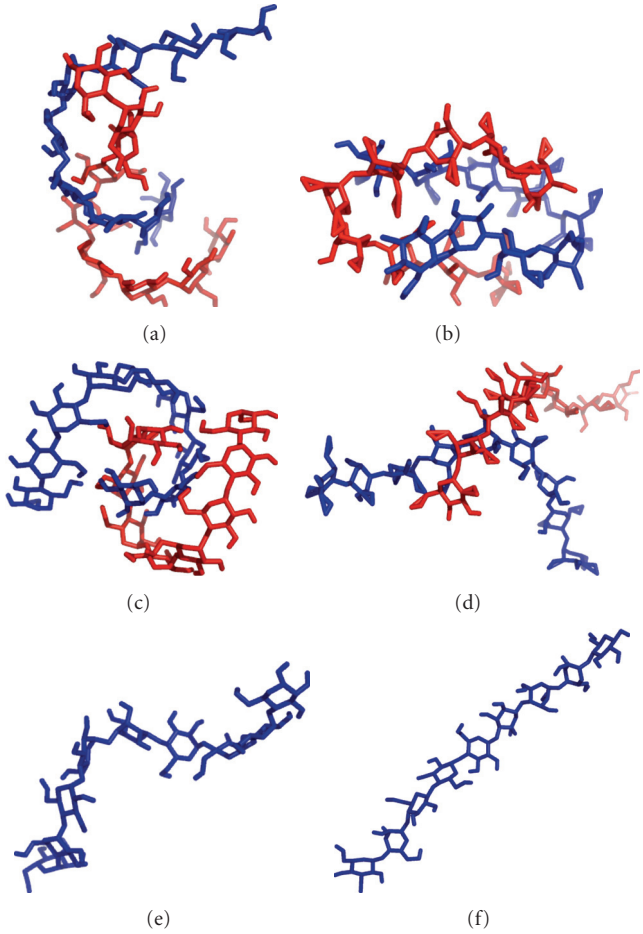

FIGURE 2: Final structures of double-stranded amylose simulated in water (amy_dou_H$_2$O (a), amy_met_dou_H$_2$O (b)) and in DMSO (amy_dou_DMSO (c), amy_met_dou_DMSO (d)), and of single-stranded amylose and cellulose in calcium sulfate solution (amy_sin_H$_2$O_caso (e), cel_sin_H$_2$O_caso (f)).

hydroxy groups maintains a helix-like structure (Figures 2(a) and 2(b)), whereas the methoxylated structure falls apart (Figures 2(a) and 2(b)).

3.2. Double-Stranded Amylose in Ionic Solution. Amylose adopts lower radii of gyration at 313 K than at 278 K (Figure 1). Hydrogen bond analysis (Table 3) shows lower hydrogen bond percentages at higher temperature, but on the other hand more favorable sulfate coordination to solute hydroxyl groups than at lower temperature. In Figure 3 the radial distribution functions for the different atom pairs are shown. The affinity of sulfate to calcium is higher at higher temperature, at least for the first solvation shell (Figure 3(a)). This suggests that the coordination of calcium and sulfate is entropy-driven. Both calcium and sulfate coordinate to the solute's hydroxyl groups that are not on the inner side of the helix (O_2 and O_3), but sulfate coordinates to a slightly larger extent than calcium. The coordination of sulfate to solute hydroxyl groups seems also to have entropic contributions; in all solvation shells higher coordination at higher temperature

Table 2: Hydrogen bond percentages (>10%) for the simulations of double-stranded amylose in pure water and in DMSO and for methylated molecules as well as for the (alchemical) molecules with excluded hydrogen bond interactions all at 313 K. (molecule number: sugar unit number: atom name).

Solute-solute hydrogen bond		Percentage hydrogen bonding				
		In water			In DMSO	
Donor atom	Acceptor atom		Excluded H-bonds	Methylated structure		Methylated structure
1 : 1 : H_3	1 : 2 : O_2	71	0	0	90	0
1 : 2 : H_3	1 : 3 : O_2	69	0	0	93	0
1 : 3 : H_3	1 : 4 : O_2	35	0	0	92	0
1 : 4 : H_3	1 : 5 : O_2	18	17	0	94	0
1 : 5 : H_3	1 : 6 : O_2	24	0	0	93	0
1 : 6 : H_3	1 : 7 : O_2	37	0	0	92	0
1 : 7 : H_3	1 : 8 : O_2	46	0	0	69	0
1 : 8 : H_3	1 : 9 : O_2	41	0	0	85	0
2 : 1 : H_3	2 : 2 : O_2	40	0	0	84	0
2 : 2 : H_3	2 : 3 : O_2	38	0	0	87	0
2 : 3 : H_3	2 : 4 : O_2	47	0	0	92	0
2 : 4 : H_3	2 : 5 : O_2	58	0	0	93	0
2 : 5 : H_3	2 : 6 : O_2	41	0	0	93	0
2 : 6 : H_3	2 : 7 : O_2	26	0	0	91	0
2 : 7 : H_3	2 : 8 : O_2	32	0	0	90	0
2 : 8 : H_3	2 : 9 : O_2	37	0	0	85	0

Table 3: Inter- and intramolecular hydrogen bond percentages (>5%) for the simulation of double-stranded amylose in ionic solution at the temperatures 278 K and 313 K. (molecule number: sugar unit number: atom name).

Hydrogen bond		Occurrence		Hydrogen bond		Occurrence	
Donor atom	Acceptor atom	278 K	313 K	Donor atom	Acceptor atom	278 K	313 K
1 : 1 : H_3	1 : 2 : O_2	77	9	1 : 1 : H_6	4 : SO_4	38	—
1 : 2 : H_3	1 : 3 : O_2	76	17	1 : 8 : H_2	1 : SO_4	48	—
1 : 3 : H_3	1 : 4 : O_2	44	27	1 : 8 : H_3	1 : SO_4	47	—
1 : 4 : H_3	1 : 5 : O_2	16	31	1 : 9 : H_2	5 : SO_4	50	—
1 : 5 : H_3	1 : 6 : O_2	19	32	1 : 9 : H_3	5 : SO_4	35	—
1 : 7 : H_3	1 : 8 : O_2	52	29	1 : 1 : H_2	1 : SO_4	—	41
1 : 8 : H_3	1 : 9 : O_2	29	29	1 : 1 : H_2	4 : SO_4	—	27
1 : 9 : H_3	1 : 9 : O_2	45	28	1 : 1 : H_3	1 : SO_4	—	25
2 : 1 : H_3	2 : 2 : O_2	77	44	1 : 3 : H_6	3 : SO_4	—	45
2 : 2 : H_3	2 : 3 : O_2	79	77	1: 4 : H_2	3 : SO_4	—	18
2 : 3 : H_3	2 : 4 : O_2	58	22	1 : 4 : H_3	2 : SO_4	—	18
2 : 4 : H_3	2 : 5 : O_2	10	37	1 : 6 : H_2	5 : SO_4	—	19
2 : 5 : H_3	2 : 6 : O_2	18	27	1 : 6 : H_3	5 : SO_4	—	38
2 : 6 : H_3	2 : 7 : O_2	37	50	1: 7 : H_2	5 : SO_4	—	13
2 : 7 : H_3	2 : 8 : O_2	35	57	1 : 7 : H_3	5 : SO_4	—	23
2 : 8 : H_3	2 : 9 : O_2	48	35	1 : 8 : H_6	5 : SO_4	—	18

was observed. Water has a higher affinity to calcium ions than to sulfate ions.

3.3. Single-Stranded Amylose and Cellulose in Ionic Solution. Figure 4 shows the radii of gyration for the simulations of single-stranded amylose and cellulose. Cellulose's radii of gyration show higher values than single-stranded amylose's. According to that observation, cellulose stays highly elongated during the simulation, whereas single-stranded amylose forms compact structures, which however show sizeable fluctuations. This is reflected in the final structures of the two molecules (Figures 2(e) and 2(f)). Neither molecule significantly changes its behavior when the temperature is

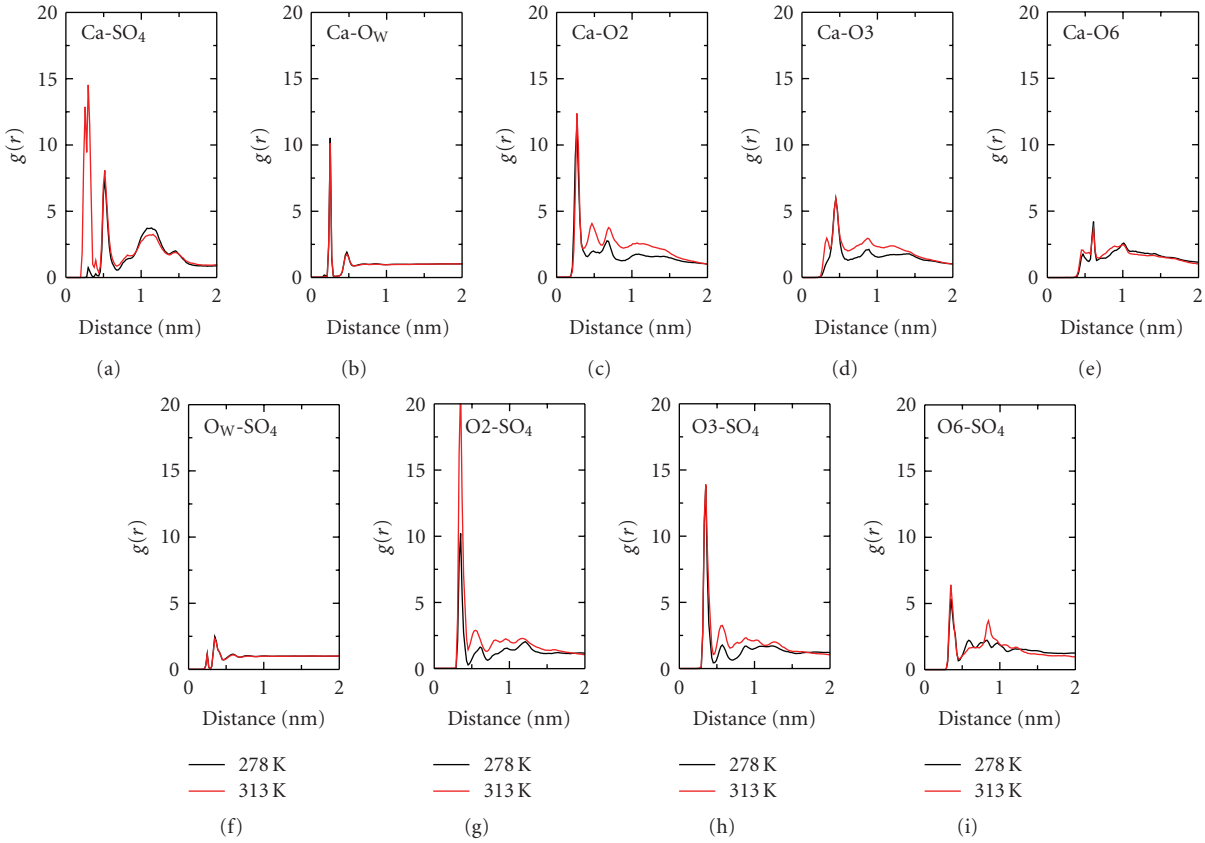

Figure 3: Radial distribution functions for different atom pairs of the simulation of double-stranded amylose in calcium sulfate solution at the two temperatures 278 K (black line) and 313 K (red line). Calcium with sulfate (A), calcium with water oxygen (B), calcium with amylose oxygen O_2 (C), calcium with amylose oxygen O_3 (D), calcium with amylose oxygen O_6 (E), sulfate with water oxygen (F), sulfate with amylose oxygen O_2 (G), sulfate with amylose oxygen O_3 (H), sulfate with amylose oxygen O_6 (I).

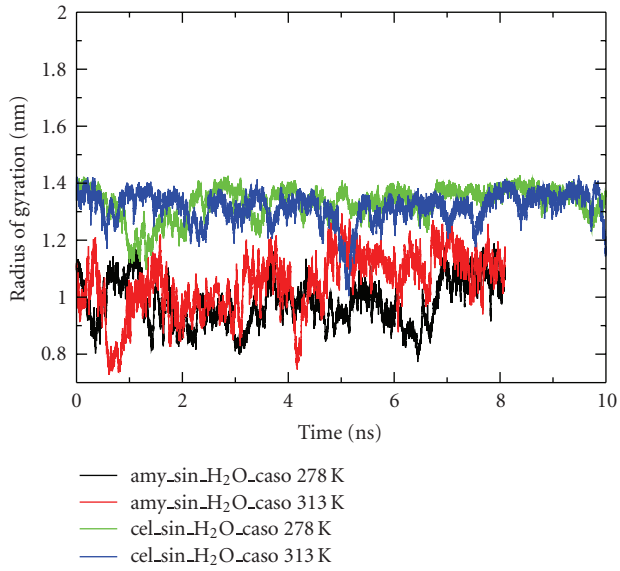

Figure 4: Radii of gyration for the ionic solutions of single-stranded amylose and cellulose at the temperatures 278 K and 313 K. Black: amy_sin_H_2O_caso at 278 K. Red: amy_sin_H_2O_caso at 313 K. Green: cel_sin_H_2O_caso at 278 K. Blue: cel_sin_H_2O_caso at 313 K.

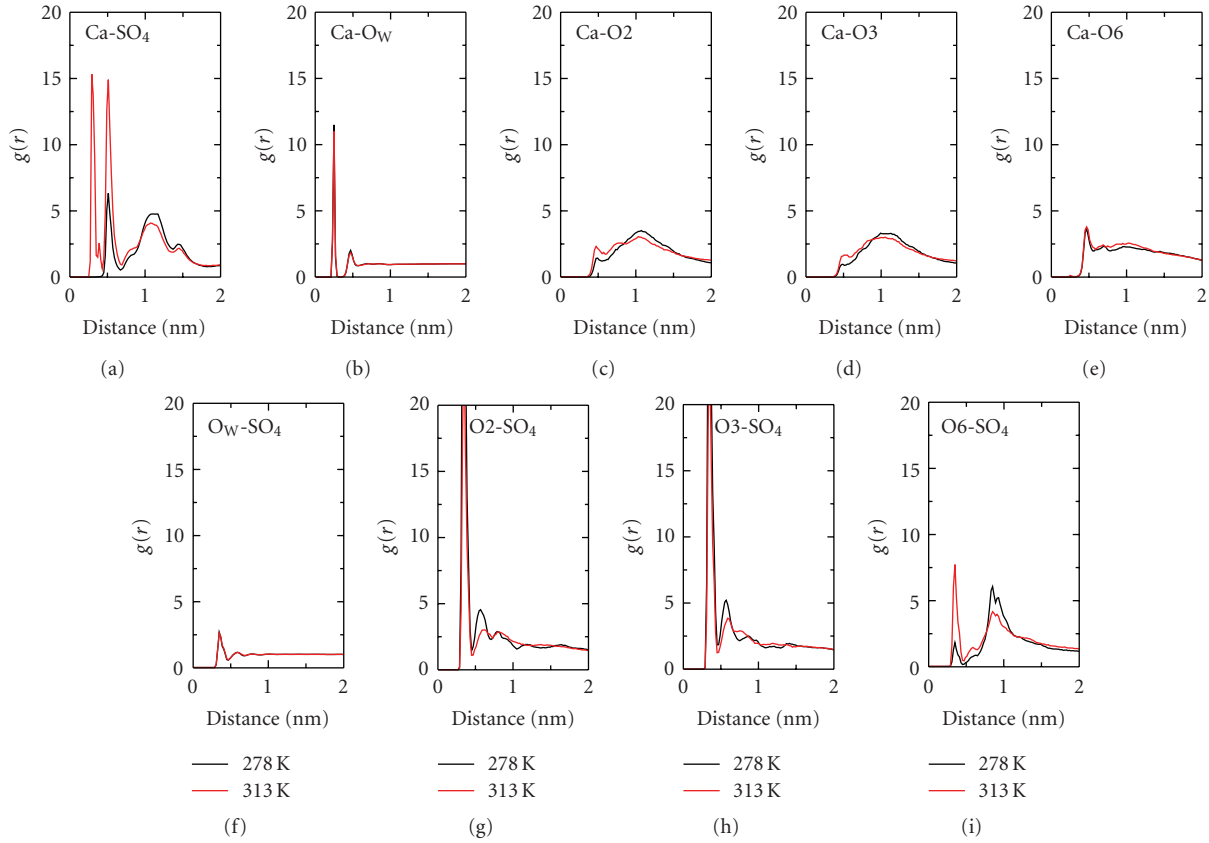

Figure 5: Radial distribution functions for different atom pairs of the simulation of single-stranded amylose in calcium sulfate solution at the two temperatures 278 K (black line) and 313 K (red line). Calcium with sulfate (a), calcium with water oxygen (b), calcium with amylose oxygen O_2 (c), calcium with amylose oxygen O_3 (d), calcium with amylose oxygen O_6 (e), sulfate with water oxygen (f), sulfate with amylose oxygen O_2 (g), sulfate with amylose oxygen O_3 (h), sulfate with amylose oxygen O_6 (i).

changed. Radial distribution functions of the two molecules are depicted in Figures 5 and 6. Comparing the coordination of calcium with sulfate, similar behavior in both simulations, of amylose and cellulose, can be observed. Both plots show higher calcium-sulfate affinity at higher temperature. Comparing the coordination of calcium and sulfate ions with solute hydroxyl groups, the two sugars show a rather different temperature dependence: the shapes of the curves in Figures 5 and 6 are similar, but in the case of amylose, ionic cordination is favoured at higher temperature, while in the case of cellulose, at lower temperature.

4. Discussion

In this work, double-stranded and single-stranded amyloses and single-stranded cellulose have been simulated under various conditions regarding solvent composition, ionic strength, and temperature. In order to observe the role of hydrogen bonds in helix formation and the formation of compact structures of double-stranded amylose, different approaches have been used to disrupt the hydrogen bond network formed by the two strands of amylose. First, the interactions between donor and acceptor atoms have been switched off; in another approach all hydroxy-groups involved in hydrogen bonds have been methylated.

From this study it can be concluded that hydrogen bonds are important for the stability of the amylose double-helix. Introducing methoxy-groups instead of hydroxy-groups hinders the formation of a helix. Changing the solvent from water to DMSO increases interstrand hydrogen bond stability which can be explained by a lack of competition between hydrogen bonds with water molecules and the hydroxy-groups of amylose. At higher temperature double-stranded amylose in calcium sulfate solution shows less interstrand hydrogen bonding and forms more compact structures. Another observation made in this work is that the coordination of calcium with sulfate is entropy-driven, and higher coordination at higher temperatures was found. Also the coordination of ions with the solute hydroxyl groups shows such behavior.

Single-stranded amylose and cellulose are similar molecules that differ in the nature of their linking glycosidic bonds. Cellulose was found to stay in an elongated conformation, whereas single-stranded amylose forms more compact structures. Another striking difference between the two molecules is the sensitivity of the coordination of ions to the solute hydroxyl groups to the temperature. The

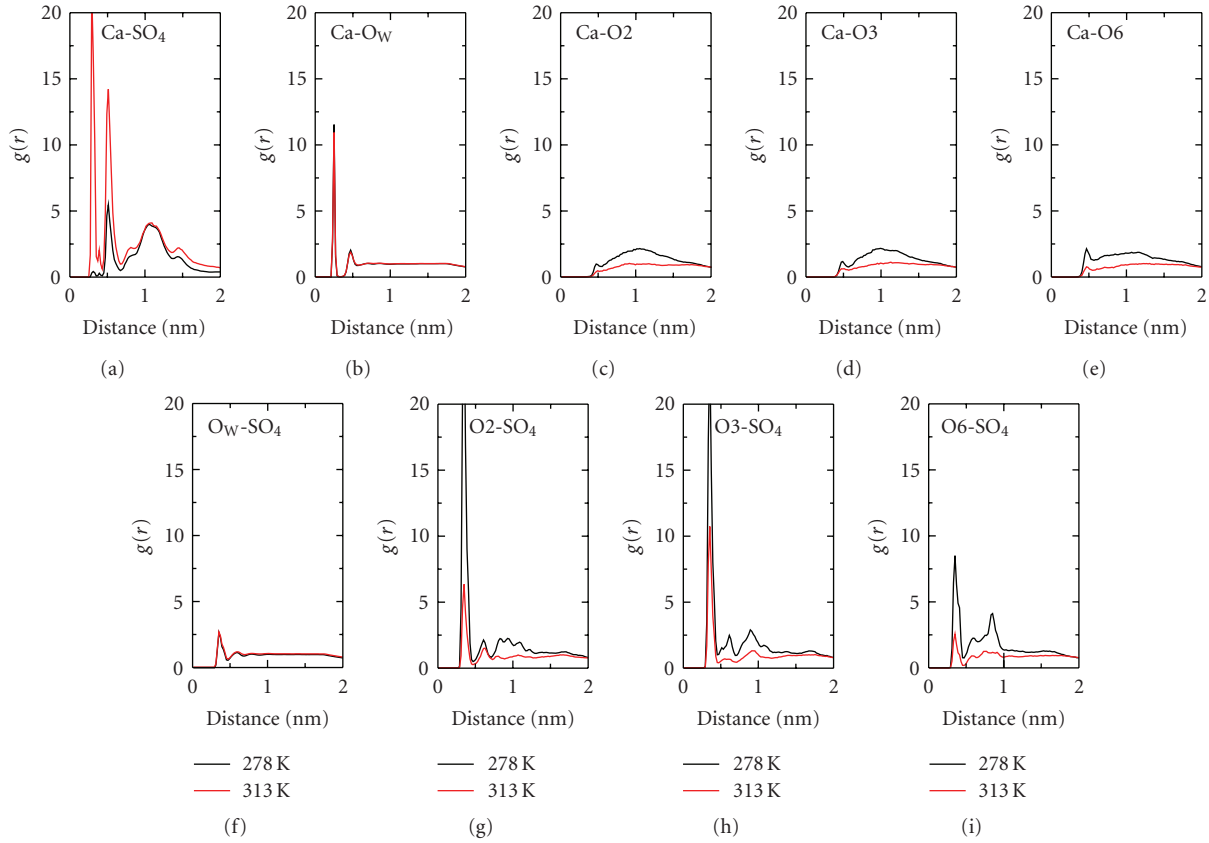

Figure 6: Radial distribution functions for different atom pairs of the simulation of cellulose in calcium sulfate solution at the two temperatures 278 K (black line) and 313 K (red line). Calcium with sulfate (a), calcium with water oxygen (b), calcium with cellulose oxygen O_2 (c), calcium with cellulose oxygen O_3 (d), calcium with cellulose oxygen O_6 (e), sulfate with water oxygen (f), sulfate with cellulose oxygen O_2 (g), sulfate with cellulose oxygen O_3 (h), sulfate with cellulose oxygen O_6 (i).

coordination of calcium and sulfate ions to solute hydroxyl groups seems to be entropy-driven in the case of amylose, whereas in the case of cellulose it is enthalpy dominated. This suggests that entropy considerations cannot be neglected when explaining the structural differences between amyloses and celluloses.

Acknowledgments

Financial support was obtained from the National Center of Competence in Research (NCCR) in Structural Biology and from Grant no. 200021-109227 of the Swiss National Science Foundation, which is gratefully acknowledged. The authors thank Cristina Pereira and Philippe Hünenberger for fruitful and inspiring discussions.

References

[1] A. Buléon, P. Colonna, V. Planchot, and S. Ball, "Starch granules: structure and biosynthesis," *International Journal of Biological Macromolecules*, vol. 23, no. 2, pp. 85–112, 1998.

[2] G. Rappenecker and P. Zugenmaier, "Detailed refinement of the crystal structure of Vh-amylose," *Carbohydrate Research*, vol. 89, no. 1, pp. 11–19, 1981.

[3] M. C. Godet, H. Bizot, and A. Buléon, "Crystallization of amylose-fatty acid complexes prepared with different amylose chain lengths," *Carbohydrate Polymers*, vol. 27, no. 1, pp. 47–52, 1995.

[4] H. Saitô, J. Yamada, T. Yukumoto, H. Yajima, and R. Endo, "Conformational stability of V-amyloses and their hydration induced conversion to B-type form as studied by high-resolution solid-state ^{13}C NMR-spectroscopy," *Bulletin of the Chemical Society of Japan*, vol. 64, no. 12, pp. 3528–3537, 1991.

[5] A. Imberty, A. Buléon, V. Tran, and S. Pérez, "Recent advances in knowledge of starch structure," *Starch-Stärke*, vol. 43, no. 10, pp. 375–384, 1991.

[6] M. B. Cardoso, J.-L. Putaux, Y. Nishiyama, et al., "Single crystals of V-amylose complexed with α-naphthol," *Biomacromolecules*, vol. 8, no. 4, pp. 1319–1326, 2007.

[7] A. C. O'Sullivan, "Cellulose: the structure slowly unravels," *Cellulose*, vol. 4, no. 3, pp. 173–207, 1997.

[8] P. Zugenmaier, "Conformation and packing of various crystalline cellulose fibers," *Progress in Polymer Science*, vol. 26, no. 9, pp. 1341–1417, 2001.

[9] Y. Nishiyama, H. Chanzy, M. Wada, et al., "Synchrotron X-ray and neutron fiber diffraction studies of cellulose polymorphs," *Advances in X-Ray Analysis*, vol. 45, pp. 385–390, 2002.

[10] J. F. Robyt, *Essentials of Carbohydrate Chemistry*, Springer, New York, NY, USA, 1998.

[11] F. Eisenhaber and W. Schulz, "Monte Carlo simulation of the hydration shell of double-helical amylose: a left-handed antiparallel double helix fits best into liquid water structure," *Biopolymers*, vol. 32, no. 12, pp. 1643–1664, 1992.

[12] H. Yu, M. Amann, T. Hansson, J. Köhler, G. Wich, and W. F. van Gunsteren, "Effect of methylation on the stability and solvation free energy of amylose and cellulose fragments: a molecular dynamics study," *Carbohydrate Research*, vol. 339, no. 10, pp. 1697–1709, 2004.

[13] W. F. van Gunsteren, S. R. Billeter, A. A. Eising, et al., *Biomolecular Simulation: The GROMOS96 Manual and User Guide*, Verlag der Fachvereine, Zürich, Switzerland, 1996.

[14] W. R. P. Scott, P. H. Hünenberger, I. G. Tironi, et al., "The GROMOS biomolecular simulation program package," *The Journal of Physical Chemistry A*, vol. 103, no. 19, pp. 3596–3607, 1999.

[15] M. Christen, P. H. Hünenberger, D. Bakowies, et al., "The GROMOS software for biomolecular simulation: GROMOS05," *Journal of Computational Chemistry*, vol. 26, no. 16, pp. 1719–1751, 2005.

[16] C. Oostenbrink, A. Villa, A. E. Mark, and W. F. van Gunsteren, "A biomolecular force field based on the free enthalpy of hydration and solvation: the GROMOS force-field parameter sets 53A5 and 53A6," *Journal of Computational Chemistry*, vol. 25, no. 13, pp. 1656–1676, 2004.

[17] R. D. Lins and P. H. Hünenberger, "A new GROMOS force field for hexopyranose-based carbohydrates," *Journal of Computational Chemistry*, vol. 26, no. 13, pp. 1400–1412, 2005.

[18] A. Imberty, H. Chanzy, S. Pérez, A. Buléon, and V. Tran, "The double-helical nature of the crystalline part of A-starch," *Journal of Molecular Biology*, vol. 201, no. 2, pp. 365–378, 1988.

[19] H. J. C. Berendsen, J. P. M. Postma, W. F. van Gunsteren, and J. Hermans, "Interaction models for water in relation to protein hydration," in *Intermolecular Forces*, B. Pullman, Ed., pp. 331–342, Reidel, Dordrecht, The Netherlands, 1981.

[20] H. Liu, F. Müller-Plathe, and W. F. van Gunsteren, "A force field for liquid dimethyl sulfoxide and physical properties of liquid dimethyl sulfoxide calculated using molecular dynamics simulation," *Journal of the American Chemical Society*, vol. 117, no. 15, pp. 4363–4366, 1995.

[21] A. Amadei, G. Chillemi, M. A. Ceruso, A. Grottesi, and A. Di Nola, "Molecular dynamics simulations with constrained roto-translational motions: theoretical basis and statistical mechanical consistency," *The Journal of Chemical Physics*, vol. 112, no. 1, pp. 9–23, 2000.

[22] J.-P. Ryckaert, G. Ciccotti, and H. J. C. Berendsen, "Numerical integration of the cartesian equations of motion of a system with constraints: molecular dynamics of *n*-alkanes," *Journal of Computational Physics*, vol. 23, no. 3, pp. 327–341, 1977.

[23] I. G. Tironi, R. Sperb, P. E. Smith, and W. F. van Gunsteren, "A generalized reaction field method for molecular dynamics simulations," *The Journal of Chemical Physics*, vol. 102, no. 13, pp. 5451–5459, 1995.

[24] A. Glättli, X. Daura, and W. F. van Gunsteren, "Derivation of an improved simple point charge model for liquid water: SPC/A and SPC/L," *Journal of Chemical Physics*, vol. 116, no. 22, pp. 9811–9828, 2002.

[25] H. J. C. Berendsen, J. P. M. Postma, W. F. van Gunsteren, A. DiNola, and J. R. Haak, "Molecular dynamics with coupling to an external bath," *The Journal of Chemical Physics*, vol. 81, no. 8, pp. 3684–3690, 1984.

[26] V. Kräutler, M. Kastenholz, and P. H. Hünenberger, "The esra molecular mechanics analysis package," 2005.